Interaction of Polypyrimidine Tract Binding Protein with the Encephalomyocarditis Virus mRNA Internal Ribosomal Entry Site†

Gary W. Witherell,*,‡ Anna Gil,§ and Eckard Wimmer‡

Department of Microbiology, State University of New York at Stony Brook, Stony Brook, New York 11794, and Center for Cancer Research and Department of Biology, Massachusetts Institute of Technology, Cambridge, Massachusetts 02139

Received December 23, 1992; Revised Manuscript Received May 6, 1993

ABSTRACT: Translation of encephalomyocarditis virus (EMCV) mRNA occurs in a cap-independent manner, requiring instead a cis-acting element termed the internal ribosomal entry site (IRES). Binding of a 57-kDa ribosome-associated protein (p57) to the EMCV IRES has been found to correlate with cap-independent translation. p57 has recently been reported to be very similar, if not identical, to the polypyrimidine tract binding protein (pPTB), a spliceosome-associated factor possibly involved in U2 snRNP/pre-mRNA complex formation or 3′-splice-site recognition. The interaction between purified pPTB and the EMCV IRES was characterized in this study using nitrocellulose filter binding and UV cross-linking assays. pPTB bound the EMCV IRES with high affinity (K_d = 40 nM at 25 °C, pH 5.5, 80 mM ionic strength). pPTB also bound strongly to RNA fragments containing either the 5′-end, 3′-end, or an internal stem–loop of the IRES. The binding properties of 16 RNA variants derived from the IRES revealed however that purified pPTB bound with less specificity than pPTB in a mixture of cytoplasmic HeLa cell polypeptides. The addition of HeLa extract to purified pPTB increased the binding specificity, suggesting that factors within the extract alter the binding specificity of pPTB. The binding of pPTB to the full-length IRES and three IRES-derived fragments was studied in detail. Complex formation was optimal at low pH and was driven entirely by entropy. As many as four ion pairs are formed upon binding, with electrostatic interactions accounting for approximately 35% of the total free energy of complex formation.

Polypyrimidine tract binding protein (pPTB) is a 57-kDa nuclear protein which has been proposed to be involved in 3′-splice-site selection and spliceosome assembly on pre-mRNA (Garcia-Blanco et al., 1989; Patton et al., 1991; Gil et al., 1991; Mulligan et al., 1992). pPTB specifically cross-links the polypyrimidine tract between the branch point and the 3′ exon (Garcia-Blanco et al., 1989; Wang & Pederson, 1990; Patton et al., 1991). Reducing the length of the polypyrimidine tract or inserting purines into the tract dramatically reduces both cross-linking efficiency and splicing activity *in vitro* (Garcia-Blanco et al., 1989; Patton et al., 1991).

Picornaviruses, a family of viruses with a single-stranded genome of plus polarity, translate their mRNA in a cap-independent manner (Jang et al., 1990). Since these viral mRNAs lack a 5′-terminal capping group, they use instead a cis-acting internal ribosomal entry site (IRES) to initiate translation. The encephalomyocarditis virus (EMCV) IRES contains approximately 600 nucleotides of the 830-nucleotide-long 5′-nontranslated region (Jang et al., 1988, 1989; Jang & Wimmer, 1990; Molla et al., 1992). Similar IRES elements have been proposed for other picornavirus mRNAs (Pelletier & Sonenberg, 1988, 1989; Kuhn et al., 1990; Brown et al., 1991), hepatitis C virus mRNA (Tsukiyama-Kohara et al., 1992), and one cellular mRNA (Macejak & Sarnow, 1991). A ribosome-associated protein (p57) has been found to specifically cross-link the EMCV IRES (Jang & Wimmer, 1990; Borovjagin et al., 1991). Mutations which disrupt the p57 binding site correlate with a dramatic decrease in cap-independent translation (Jang & Wimmer, 1990), an observation suggesting that p57 binding is required for translation of EMCV mRNA. On the basis of similarities in purification characteristics and protease cleavage patterns, p57 has been found to be very similar, if not identical, to pPTB (Hellen et al., 1993). This surprising result was corroborated by the observation that anti-pPTB antibodies inhibit cap-independent translation of encephalomyocarditis virus mRNA but not cap-dependent translation of β-globin mRNA (Hellen et al., 1993).

In this paper the interaction between pPTB and the EMCV IRES is studied using nitrocellulose filter binding and UV cross-linking assays. The results show that purified pPTB binds the EMCV IRES and several fragments of the IRES with high affinity but lower specificity than endogenous pPTB in crude cellular extracts. The addition of cellular extract to purified pPTB was found to increase the binding specificity. Binding of pPTB to RNA was found to be entirely entropy-driven, stabilized by ionic interactions, and required protonation of a titratable group with a pK near 6 for optimal binding.

EXPERIMENTAL PROCEDURES

Materials. Oligodeoxynucleotides were synthesized on an Applied Biosystems 380B DNA synthesizer. Calf intestine alkaline phosphatase, RNAse T1, and RNA homopolymers were purchased from Boehringer Mannheim. T7 DNA polymerase (Sequenase) was purchased from U.S. Biochemical Corp., and Taq DNA polymerase was purchased from Perkin-Elmer Cetus. DNA restriction enzymes, T4 DNA ligase, and DNA polymerase I (Klenow fragment) were purchased from New England Biolabs. Manufacturer's protocols were followed for all reactions. [α-^{32}P]UTP (3000 Ci/mmol), [^{35}S]-dATP, and [γ-^{32}P]ATP were purchased from Amersham.

Plasmids. Plasmids were constructed by introducing deletions or insertions into plasmid vectors pBS-ECAT (Jang

† This work was supported by National Institutes of Health Grants AI-15122 and AI-32100 to E.W. and by National Institutes of Health Postdoctoral Fellowship AI-08482 to G.W.

‡ SUNY at Stony Brook.

§ MIT.

0006-2960/93/0432-8268$04.00/0 © 1993 American Chemical Society

et al., 1988) and pBS-ECAT393 (Jang & Wimmer, 1990) to create transcription templates for RNA fragments. *Sty*I, *Eco*RI, and *Apa*II restriction sites blunt-ended with Klenow fragment of DNA polymerase I are indicated by (blunt). Oligonucleotide A was amplified by the polymerase chain reaction (PCR) from pBS-ECAT using primers TAACCTAGGGGTCTTTCCCCTAGGAATGCAAGGTCT and GGATATATCAACGGTGG. Mispriming resulted in the deletion of the sequence underlined. Plasmid template for fragment 12 was created by ligating *Sty*I–*Pst*I and *Bst*XI–*Pst*I fragments of pBS-ECAT393 with *Sty*I- and *Bst*XI-digested oligo A. Oligonucleotide B was PCR-amplified from pBS-ECAT using primers CCCGAATTCGAGCTCTAACGTTACTGGCCG and ATTGGGCCCTCGGTGGAAAATACATATAG. Fragments of plasmid pBS-ECAT (*Apa*I–*Nco*I- and *Eco*RI–*Nco*I-digested) were ligated to oligo B (*Eco*RI–*Apa*I digested) to construct plasmid template for fragments 5, 6, and 7. Plasmid template for fragment 16 was created by ligating together *Eco*RI(blunt)–*Pst*I and *Apa*II(blunt)–*Pst*I fragments of pBS-ECAT. Restricted plasmid pBS-ECAT was used directly as template for fragments 1, 2, and 3. Restricted plasmid pBS-ECAT393 was used directly as template for fragment 8. Plasmids pBS-ECAT403M2 and pBS-ECAT403M1 (Jang & Wimmer, 1990) were used directly as templates for fragments 9 and 10, respectively. Following complete digestion with restriction enzymes, the DNA fragments were purified on low melting point agarose gels (Sambrook et al., 1989) and ligated with T4 DNA ligase. *Escherichia coli* C600 was used as a host in each case (Bachmann 1987; Raleigh et al., 1988). Transformants harboring plasmid DNA were screened by ampicillin resistance and restriction analysis of minilysate plasmid DNA (Sambrook et al., 1989). Plasmids were sequenced in the region of interest with T7 DNA polymerase using ^{35}S-labeled dATP.

RNAs. Oligoribonucleotides were prepared by *in vitro* transcription from synthetic DNA (fragments 4 and 13), from PCR templates amplified using a 5′ primer containing a T7 promoter (fragments 11, 14, and 15), or from restricted CsCl-purified (Sambrook et al., 1989) plasmid DNA (fragments 1–3, 5–10, 12, and 16) by procedures previously described (Milligan et al., 1987; Sampson & Uhlenbeck, 1988). RNAs were labeled by the addition of [α-^{32}P]UTP (5 μCi) into the transcription reaction. RNAs for filter binding assays were gel-purified by electrophoresis on denaturing 6% or 10% polyacrylamide gels; the RNA was electroeluted out of the gel, ethanol-precipitated, and stored in 10 mM Tris/0.1 mM EDTA, pH 8.0, at −20 °C. For UV cross-linking assays, transcription reactions were purified using Stratagene NucTrap push columns and a 5 mM Hepes, pH 7.6, 25 mM KCl, 5 mM $MgCl_2$, and 0.1 mM EDTA elution buffer.

Homopolymers were 5′-end-labeled by removing the 5′ triphosphate with calf intestine phosphatase followed by 5′ ^{32}P labeling with T4 polynucleotide kinase and [γ-^{32}P]ATP (Sambrook et al., 1989). Homopolymers were purified using Stratagene NucTrap push columns and a 5 mM Hepes pH 7.6, 25 mM KCl, 5 mM $MgCl_2$, and 0.1 mM EDTA elution buffer.

Polypyrimidine Tract Binding Protein and Preparation of HeLa Extract. Recombinant pPTB, containing at the amino-terminus 12 vector-derived amino acids, was purified from *E. coli* (according to A. Gil and P. Sharp, unpublished results). HeLa extract was prepared as described previously (Molla et al., 1991) except that dialysis and micrococcal nuclease steps were omitted. HeLa extract was adjusted to 10% (v/v) glycerol and strored at −80 °C.

Filter Binding Assays. Protein excess filter binding assays were performed under various buffer and temperature conditions described in text. Typical 25-μL reactions contained MMK buffer (50 mM MES, pH 5.5, 10 mM KCl, and 5 mM MgOAc) and were incubated at 25 °C for 10–30 min before filtration. Reactions were filtered through Schleicher and Schuell nitrocellulose filters (0.45-μm pore size) presoaked in MMK buffer. The filters were then washed with 200 μL of MMK buffer, dried in scintillation vials for 20 min at 190 °C, and counted in Econolume. All RNAs were heated to 95 °C for 3 min and quick-cooled on ice just before use. Backgrounds obtained in the absence of protein were less than 5% of the input radioactivity and subtracted in all cases. Filtration assays contained ^{32}P-labeled RNA (~10 pM) and pPTB concentrations from 5 to100 nM. Retention efficiencies of the RNA ranged from 40% to 60%. Equilibrium binding constants varied less than a factor of 2 for independent replicates.

Cross-Linking Assays. Ultraviolet light (UV) cross-linking assays were performed as described previously (Jang & Wimmer, 1990). ^{32}P-Labeled RNAs (~50 pM) were incubated with either 0.3 μg of purified pPTB (20 μM), 50 μg of HeLa extract, or both in 30 μL of MMK buffer containing 1 μg of rRNA at 25 °C for 15 min. Reactions were cross-linked in a Stratagene Stratalinker 2400 UV cross-linker at 4000 μW/cm^2 for 40 min. RNAs were digested by incubation with 20 μg of RNase A and 200 units of RNase T1 at 37 °C for 1 h. Cross-linked proteins were separated on 12.5% sodium dodecyl sulfate (SDS) polyacrylamide gels using the buffer system of Laemmli (1970), as modified by Nicklin et al. (1987). Gels were electrophoresed at 5–10 V/cm at constant current (70 mA), dried, and autoradiographed.

RNA Folding. Optimal and suboptimal foldings for RNA sequences were computed using the MFOLD package by Zuker and Jaeger (Zuker, 1989; Jaeger et al., 1989, 1990). All of the secondary structures illustrated were the optimal foldings except fragments 8 and 12, which were within 0.2 kcal (0.8%) and 0.1 kcal (0.6%), respectively, of the optimal structure.

RESULTS

Binding of pPTB to the EMCV IRES. Protein–RNA complexes were formed by incubating pPTB and the EMCV IRES (Figure 1A) together in MMK buffer at 25 °C for 10–20 min and detected by retention on a nitrocellulose filter. EMCV IRES refers to the 3′-terminal segment (nt 260–840) of the 5′-nontranslated region (NTR) of the EMCV genome containing at the 5′ end a 24-nt-long polypyrimidine tract. This polypyrimidine tract originates from the poly(C) tract found in the 5′ NTR of most cardioviruses. The 3′ border of the EMCV IRES is the AUG which initiates polyprotein synthesis (Jang et al., 1990). Figure 2 shows a typical protein excess assay in which a constant, low concentration (~50 pM) of ^{32}P-labeled RNA is incubated with varying concentrations of pPTB. The protein concentration at half-saturation is equal to the equilibrium dissociation constant (K_d) for the reaction, assuming a stoichiometry of 1 and 100% active protein in RNA binding. Binding data to the EMCV IRES fit a simple bimolecular binding curve with K_d = 40 nM (Figure 2). Binding of pPTB to a 50-nucleotide-long RNA transcribed from pGEM9Z-1 vector (Promega) could not be detected (K_d > 200 nM) (Figure 2). Polyuridine, polycytidine, polyadenosine, and polyguanosine were also unable to bind pPTB within the detection limit of the assay (Table I). Garcia-

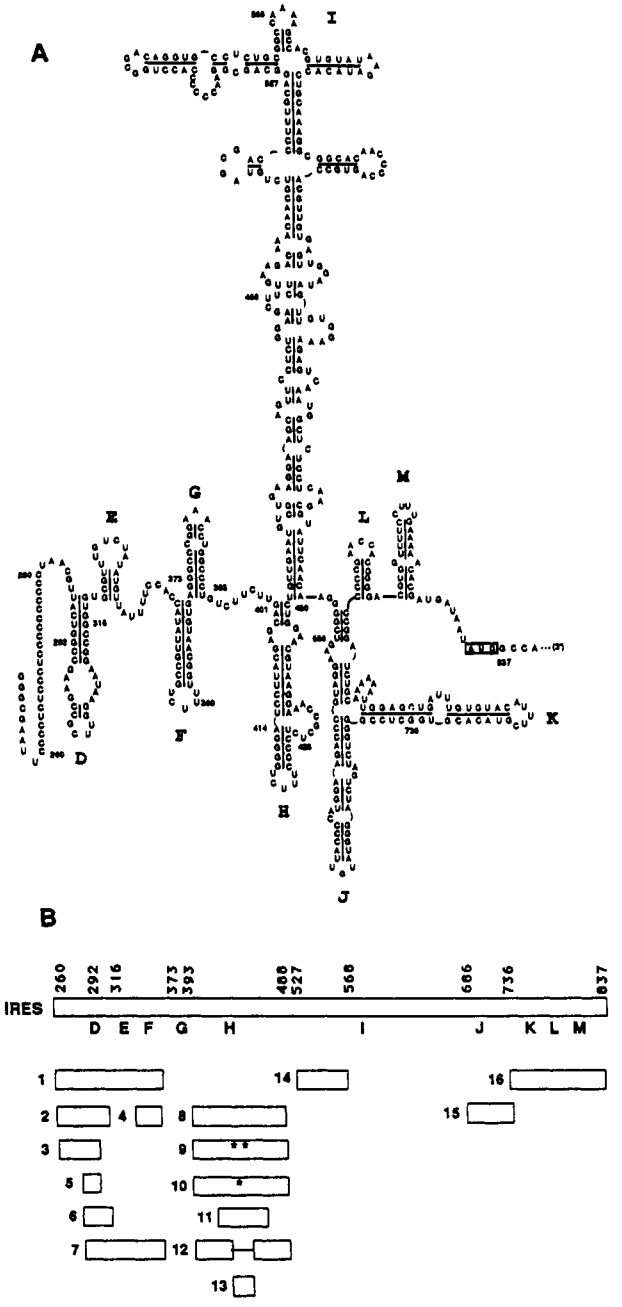

FIGURE 1: (A) Schematic representation of predicted secondary structure of the EMCV IRES (Pilipenko et al., 1989; Duke et al., 1992). Stem–loop structures are sequentially named by letters according to Duke et al. (1992) and nucleotide positions on the EMCV genome are marked by numbers. The initiating AUG start codon is boxed. (B) Linear representation of EMCV IRES and IRES fragments used for UV cross-linking studies. Numbers above the IRES correspond to nucleotide positions on EMCV mRNA, while letters below the IRES correspond to the position of stem–loop structures shown in panel A. IRES fragments are identified by number and positioned below the full-length IRES to show relation of fragment sequences to IRES sequence. Sequence differences between the fragment sequences and the full-length IRES are indicated by asterisks, and deletions are indicated by lines.

Blanco et al. (1989) have observed that neither polyuridine, polyinosine, nor poly(AUC) is able to compete efficiently with pPTB binding to the Ad10 splicing precursor.

Binding of pPTB to 5′-Fragments of the EMCV IRES. The EMCV IRES is approximately 600 nt long (Jang & Wimmer, 1990) and contains, following the 24-nt polypyrimidine tract, a series of stem–loop structures designated D–M, Figure 1A). To determine where on the EMCV IRES pPTB

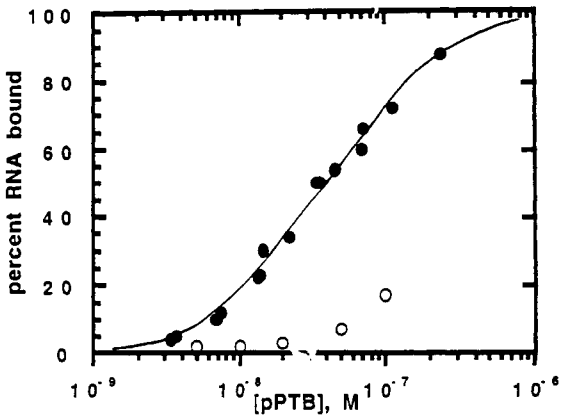

FIGURE 2: Protein excess binding curve for pPTB and either full-length EMCV IRES RNA (●) or a 50-nt pGEM9Z-1 (Promega) vector RNA (O). Binding was assayed in MMK buffer, pH 5.5, 25 °C at various protein concentrations (5–100 nM). The solid line is a theoretical binding curve calculated using K_d = 40 nM, assuming a stoichiometry of 1 and 100% active protein.

Table I: Binding Affinities of RNA Fragments to pPTB

fragment	K_d (nM)	fragment	K_d (nM)
EMCV IRES	40	6	71
PGEM9Z-1	>200	7	21
poly(U)	>200	8	20
poly(C)	>200	9	14
poly(A)	>200	10	40
poly(G)	>200	11	24
1	20	12	100
2	25	13	>200
3	30	14	71
4	>200	15	77
5	>200	16	31

bound, fragments of the IRES were synthesized (Figure 1B). Fragments tested for pPTB binding contained sequence from the 5′ polypyrimidine tract (fragment 3), D-loop (fragment 2, fragment 6), DE-loops (fragment 7), DEF-loops (fragment 1), F-loop (fragment 4), H-loop (fragments 8–13), I-loop (fragment 14), J-loop (fragment 15), and KLM-loops including the initiation codon (fragment 16). Possible secondary structures of these RNA fragments are shown in Figure 3, and K_d values measured under standard assay conditions (see Materials and Methods) are shown in Table I.

pPTB bound an RNA fragment derived from the 5′-end of the EMCV IRES (fragment 1, K_d = 20 nM) with twice the affinity of the full-length IRES. Fragment 1 contains sequence from the 5′ polypyrimidine tract and the DEF-loops. To localize the pPTB binding site further, 3′ deletions in fragment 1 were made. Deletion of nucleotides corresponding to part of the EF-loop (fragment 2, K_d = 25 nM) or DEF-loop (fragment 3, K_d = 30 nM) had little effect on binding. The F-loop sequence alone (fragment 4, K_d > 200 nM) failed to bind pPTB. Apparently, D-, E-, and F-loop sequences do not augment pPTB binding to fragment 1. Fragment 1 and the two deletion fragments (fragments 2 and 3) have in common the 24-nt polypyrimidine tract at the 5′ end of the IRES. This polypyrimidine tract is a likely pPTB binding target since many pPTB cross-linking sites contain polypyrimidine tracts of 10 or more nucleotides (Garcia-Blanco et al., 1989; Wang & Pederson, 1990; Patton et al., 1991). To determine whether the polypyrimidine tract was indeed responsible for pPTB binding to these fragments, 19 nt of the polypyrimidine tract in fragment 3 was replaced with 5 nt of linker sequence (fragment 5, K_d > 200 nM). As expected, this mutation reduced binding greater than 6-fold, below the detection limit of the assay. Surprisingly, the same substitution in fragment

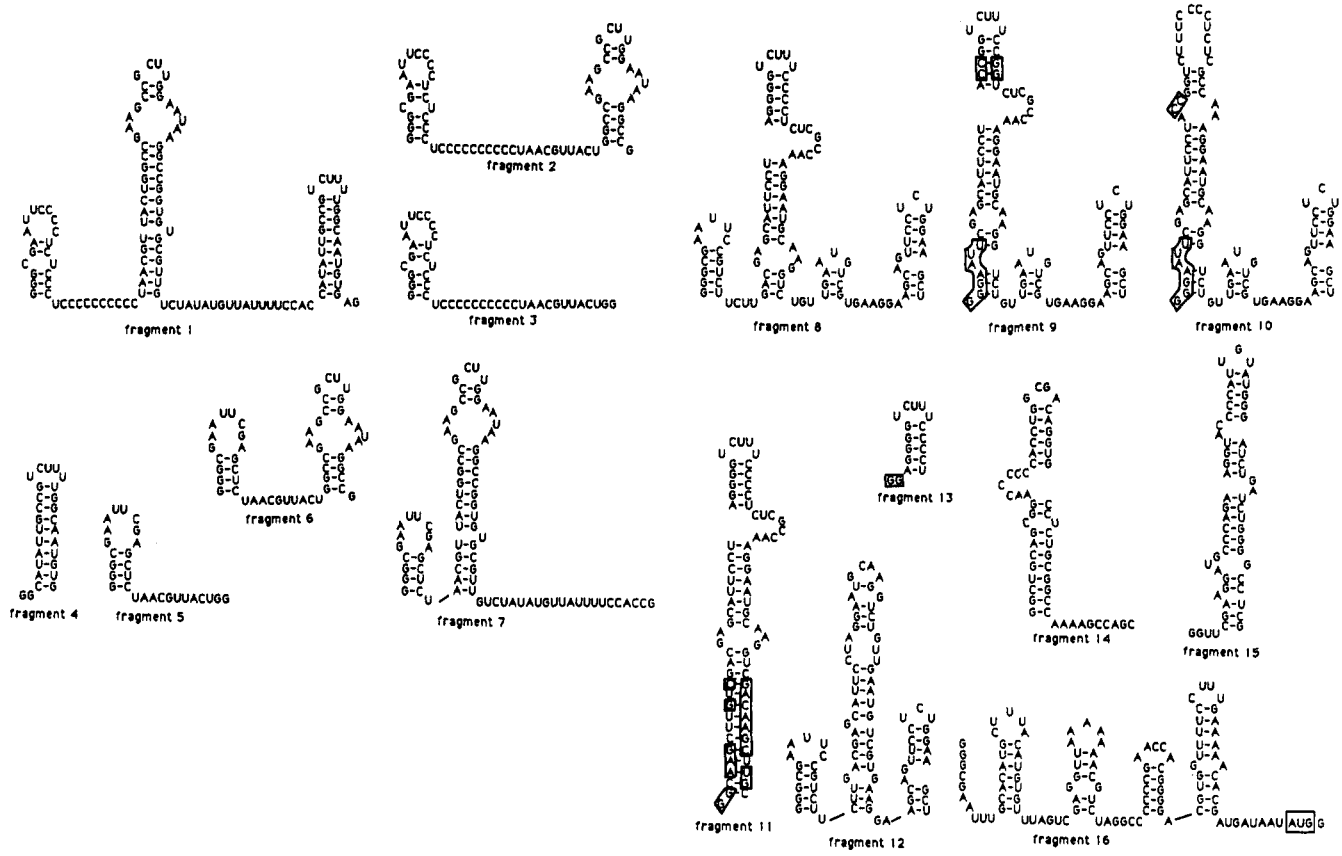

FIGURE 3: RNA fragments and variants derived from the EMCV IRES. Sequences and possible secondary structures of RNA fragments 1–16 derived from either the 5′-end of the EMCV IRES (fragments 1–7), the H-loop (fragments 8–13), or the 3′-end of the EMCV IRES (fragments 14–16). Differences between fragments 9–13 and fragment 8 are boxed. The EMCV initiation codon is boxed in fragment 16.

2 (fragment 6, K_d = 71 nM) reduced binding only 3-fold and the substitution in fragment 1 (fragment 7, K_d = 21 nM) had no effect on pPTB binding. These results suggest that the 5′ polypyrimidine tract is not required for pPTB binding to the 5′-end of the EMCV IRES.

Binding of pPTB to Sequences Related to H-Loop. The observation that pPTB is very similar, if not identical, to p57 led us to test whether purified pPTB would bind the same RNAs which cross-link pPTB/p57 in a crude mixture of cytoplasmic polypeptides. The best studied pPTB/p57 cross-linking sites contain sequence derived from the EMCV IRES H-loop (Jang & Wimmer, 1990). Using the nitrocellulose filter binding assay, purified pPTB was found to strongly bind an RNA fragment containing H-loop sequence (fragment 8, K_d = 20 nM) and a sequence variant of H-loop (fragment 9, K_d = 14 nM). Both of these fragments, whose sequence and possible secondary structures are shown in Figure 3, cross-link endogenous pPTB/p57 in rabbit reticulocyte lysate (RRL) well (Jang & Wimmer, 1990). An H-loop sequence variant, which was designed to disrupt the upper stem of H-loop (Figure 3, fragment 10), did not UV cross-link endogenous pPTB/p57 in RRL efficiently (Jang & Wimmer, 1990). Surprisingly, this fragment was able to bind purified pPTB with only a 2-fold lower affinity (K_d = 40 nM), a phenomenon further analyzed below.

To localize the pPTB binding site on H-loop sequences further, the binding affinity of pPTB to three other RNAs was determined (fragments 11–13, Figure 3, Table I). Replacing the three small stem–loops in fragment 8 and extending the long stem–loop had no effect on binding (fragment 11, K_d = 24 nM). The importance of the upper stem was assayed with fragments 12 and 13 . Deleting the entire upper stem–loop (fragment 12, K_d = 100 nM) reduced binding approximately 5-fold, while the upper stem–loop itself was unable to bind pPTB (fragment 13, K_d > 200 nM).

Binding of pPTB to I-Loop, J-Loop, and the 3′-End of the IRES. pPTB bound sequences derived from the I-loop (fragment 14 , K_d = 71 nM) and J-loop (fragment 15, K_d = 77 nM) only weakly (Figure 3, Table I). pPTB did, however, bind very well to a 110-nt long RNA fragment (fragment 16, K_d = 31 nM) containing sequence from the 3′-end of the IRES, which includes the initiation codon. This sequence contains a short (9 nt) polypyrimidine tract (Figure 3) and shows no sequence or structural homology to any of the other RNA fragments which bind pPTB.

Cross-Linking of pPTB to IRES Fragments. As an alternative method for determining the binding specificity of pPTB, cross-linking assays were performed (Figure 4A). As expected, RNA fragments which bound strongly, K_d < 70 nM, (EMCV IRES and fragments 1, 2, 7–10, and 16) cross-linked strongly, while RNA fragments with low affinity, K_d > 75 nM, (fragments 4, 13, and 15) cross-linked weakly. Fragments 6 and 14, with moderate affinities of 71 nM, cross-linked either strongly (fragment 6) or weakly (fragment 14). For two RNAs, however, the intensity of the cross-linking signal was much weaker (fragment 11) or much stronger (fragment 12) than expected on the basis of the filter binding affinity (Table I). Differences between results with filter binding and cross-linking assays could be due to the use of an *E. coli*-expressed recombinant protein in filter binding assays, which may be deficient in posttranslational modifications. Alternatively, the differences could be due to limitations of the cross-linking assay. Cross-linking assays do not directly measure binding affinity, as filter binding assays do, since the cross-linking signal is determined not only by the affinity of a protein for its binding target but also by the number of sites

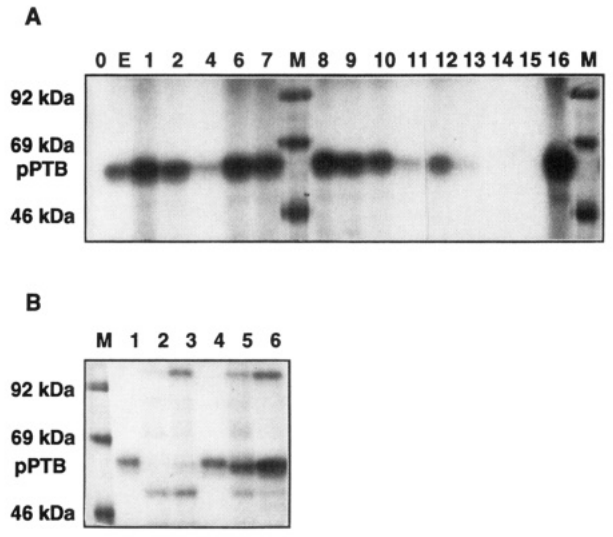

FIGURE 4: UV cross-linking of pPTB and various RNA fragments derived from EMCV IRES. Cross-linking assays were performed in MMK buffer, pH 5.5, at 25 °C and contained 0.2 μM pPTB and ^{32}P-labeled RNA. Reactions were UV cross-linked, digested with ribonucleases, and run on SDS–polyacrylamide gels. Bands corresponding to pPTB and protein markers of 92, 68, and 42 kDa (lane M) are labeled. (A) Lane 0, no pPTB; lane E, EMCV IRES; lanes 1–16 , fragments 1–16 , respectively, shown in Figure 3. (B) Lanes 1–3, fragment 10 with either pPTB, HeLa extract, or both, respectively; lanes 4–6, fragment 8 with either pPTB, HeLa extract, or both, respectively.

cross-linked, the location of the protein cross-linking site(s) relative to a labeled nucleotide, the number of labeled nucleotides protected against ribonuclease digestion by the cross-linked protein, and the particular amino acid that contacts the RNA (since aromatic and heterocyclic amino acids, as well as cysteine, are especially photoreactive). The cross-linking signal may be altered so drastically by these effects that an RNA labeled with one nucleotide will appear to bind strongly while the same RNA labeled with a different nucleotide will appear to bind weakly (G. W. Witherell and E. Wimmer, unpublished results). Thus fragment 11 likely binds well but does not cross-link well, while fragment 12 likely binds weakly but cross-links strongly. Considering the limitations of the cross-linking assay, the cross-linking intensities and filter binding affinities are reasonably consistent overall, suggesting that the cross-linking signal for these RNAs is primarily determined by the affinity of the protein for the RNA. However, conclusions on the extent of interaction between protein and RNA based solely on the UV cross-linking properties of labeled RNA fragments must be made with caution.

So far we have tested only the binding of purified pPTB to RNA. It is possible, however, that the binding specificity is altered if pPTB is incubated with RNA in the presence of other proteins. We tested this possibility by cross-linking purified pPTB, HeLa cell extract, or a mixture of both with fragments 8 and 10 (Figure 4B). Fragment 10 was chosen since it UV cross-links purified pPTB with a moderate intensity (Figure 4A, lane 10; Figure 4B, lane 1), whereas in experiments with RRL this fragment cross-linked endogenous pPTB/p57 poorly (Jang & Wimmer, 1990). Interestingly, neither endogenous pPTB/p57 contained in a crude HeLa extract (Figure 4B, lane 2) nor purified pPTB mixed with HeLa extract (Figure 4B, lane 3) cross-linked fragment 10 efficiently. In contrast, fragment 8 readily cross-linked purified pPTB (Figure 4B, lane 4), endogenous pPTB/p57of a crude HeLa extract (Figure 4B, lane 5), and purified pPTB mixed with HeLa extract (Figure 4B, lane 6). Mixing purified pPTB and HeLa extract in fact enhances pPTB cross-linking to fragment 8 (lane 6). The size difference between purified pPTB and endogenous pPTB/p57 is due to 12 vector-derived amino acids contained in the recombinant pPTB (see Materials and Methods). It is also noteworthy that the addition of pPTB to the HeLa extract enhances cross-linking of a 100-kDa polypeptide to both fragments (Figure 4B, lanes 3 and 6). pPTB and a protein with a molecular weight of 100 kDa have been proposed to exist as part of a large complex that is required to rescue splicing from depleted nuclear extracts (Patton et al., 1991). It is uncertain, however, whether the cytoplasmic 100-kDa protein observed here and the nuclear 100-kDa protein described by Patton et al. (1991) are identical proteins.

Solution Properties of pPTB Binding. The solution properties of pPTB binding to two different RNA fragments (fragments 1 and 7) are shown in Figure 5. Fragments 1 and 7, with nearly identical affinities for pPTB (Table I), share 68% nucleotide sequence homology but differ structurally (Figure 3). Moreover, they are distinct through the lengths of their polypyrimidine tracts of 24 nt (fragment 1) and 6 nt (fragment 7). The pH dependence of the equilibrium association constant ($K_a = 1/K_d$) was measured by substituting the standard MES buffer with a buffer having an appropriate pK_a. The two pPTB–RNA interactions both show a similar pH optimum below pH 5.5 (Figure 5A). The pH dependence indicates that some functional group(s) with a pK near 6, possibly histidine, must be protonated for optimal binding to both RNAs.

The temperature dependence of K_a was obtained by performing standard filter binding assays at various temperatures. A van't Hoff plot of the data ($\ln K_a = -\Delta H/RT$) is shown in Figure 5B. The ΔH obtained from the slope of the line is +0.7 kcal/mol for fragment 1 and +2.63 kcal/mol for fragment 7; thus, ΔH is unfavorable for complex formation in both cases. Favorable ΔS values are calculated to be +36.6 and +42.3 cal/(K·mol of complex) for fragments 1 and 7, respectively, at 25 °C. Complex formation is therefore driven solely by entropy in both cases.

The ionic strength dependence of K_a was determined by performing standard filter binding assays in which KCl was added to give the indicated cation concentration. Figure 5C shows that K_a decreases with increasing ionic strength for both fragments 1 and 7, indicating that there are ionic interactions involved in complex formation. Record and coworkers have developed a quantitative analysis of the salt dependence of K_a for DNA–protein interactions based on ion displacement (Record et al., 1976). Calculation of the number of ion pairs (m') formed in the interaction is made using the equation $\log K_a = m'\psi \log [M^+]$, where ψ is the fraction of counterions (M^+) bound per phosphate of the RNA fragment. Because application of this analysis to RNA–protein interactions requires several untested assumptions, the number of ion pairs determined is considered to be an upper limit. From the slope of Figure 5C, 3.4 and 3.5 ion pairs are formed between the protein and fragments 1 and 7, respectively, when ψ is assumed to be 0.85, as for the R17 synthetic operator (Carey & Uhlenbeck, 1983). Thus, four or less nucleotide phosphates on each RNA are involved in ion pairs with cationic groups on the protein. The nonelectrostatic contribution to the total free energy of the interaction can be calculated from the extrapolated value of K_a at 1 M salt and the equation ($\Delta G_{\text{nonelect}} = \Delta G_{1M} - m'\Delta G_{\text{lys-phosphate}}$). It has been estimated that at 1 M salt each lysine–phosphate-type ion pair contributes about +0.2 kcal/mol (Lohman et al., 1980). Thus, using this

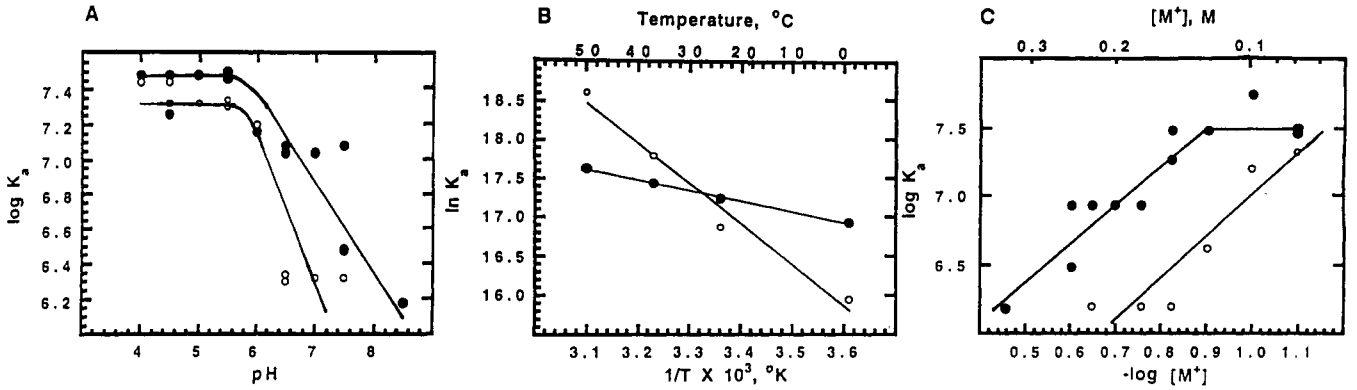

FIGURE 5: pH, temperature, and ionic strength dependence of pPTB binding to fragment 1 (●) and fragment 7 (○). (A) pH dependence of K_a. Standard filtration assays were performed with either NaOAc (pH 4.0, 4.5, and 5.0), MES (pH 5.5, 6.0, and 6.5), MOPS (pH 7.0 and 7.5), or Tris (pH 8.0 and 8.5) buffers. (B) Temperature dependence of K_a. Standard filtration assays were performed with the temperature adjusted as indicated. The slopes of the lines correspond to ΔH = +0.7 and +2.6 kcal/mol of complex. (C) Ionic strength dependence of K_a. Standard filtration assays were performed with the KCl concentration adjusted to give the total cation concentration [M^+] indicated. The slope of the line corresponds to 3.6 and 3.5 ion pairs formed between the protein and the two RNAs, respectively.

estimate for the four ion pairs formed between the protein and RNA and an extrapolated value of ΔG = –6.5 kcal/mol at 1 M salt, the nonelectrostatic contribution to ΔG is –7.3 kcal/mol for fragment 1. This is approximately 71% of the total free energy of the interaction under standard assay conditions. A similar analysis of complex formation with fragment 7 (ΔG = –5.5 kcal/mol) reveals a nonelectrostatic contribution to ΔG of –6.3 kcal/mol, approximately 63% of the total free energy of the interaction under standard assay conditions. Thus ionic interactions contribute less than 40% of the total free energy in both complexes.

Similar solution properties were obtained for pPTB binding to fragments 8 and 9 and the EMCV IRES (data not shown). Thus, four IRES fragments and the full-length IRES bind pPTB with very similar solution properties.

DISCUSSION

A filter binding assay for pPTB permits the binding affinities of pPTB for various RNAs to be determined and the solution properties to be measured. The proposal that pPTB, a protein predominantly resident in the nucleus of HeLa cells (Ghetti et al., 1992), is involved in cap-independent translation of picornavirus mRNA suggested that it would bind the EMCV IRES. Using the nitrocellulose filter binding assay, we have shown that pPTB binds the EMCV IRES with high affinity. Three RNA fragments derived from the 5′-end, the H-loop, and the 3′-end of the IRES also bind pPTB with high affinity. These results are in agreement with the observation that pPTB in crude cell extracts can be UV cross-linked to these same RNA fragments (Jang & Wimmer, 1990; G. W. Witherell and E. Wimmer, unpublished results). Whether pPTB binds to these same regions in the full-length IRES is unknown since it is possible that the recognition features on the fragments are drastically altered in the context of the full-length IRES. The stoichiometry of pPTB binding to the full-length IRES has not yet been determined.

The binding specificity of pPTB for the IRES fragments did not suggest any primary sequence element within these regions that pPTB recognizes. Although the three regions of the IRES (represented by fragments 1, 8, and 16) which bind pPTB strongly contain polypyrimidine tracts from 9 to 24 nt in length, binding affinity does not correlate with the length of the polypyrimidine tract. Indeed, our data suggest that a polypyrimidine tract greater than or equal to 10 nt in length is neither sufficient (as for fragment 13) nor necessary (as for fragments 7, 9, and 16) for pPTB binding. The binding of pPTB to the 3′-terminal fragment of the EMCV IRES (fragment 16) may reflect a report that a protein with a molecular mass of 57 kDa (presumed to be pPTB) cross-links the 3′-terminal fragment of the foot and mouth disease virus (FMDV) IRES (Luz & Beck, 1991). The FMDV IRES is predicted to fold with a secondary structure similar to that of the EMCV IRES (Pilipenko et al., 1989). However, the authors found binding of endogenous p57 to the 3′-terminal fragment of the FMDV IRES only at low salt concentrations.

pPTB has been found to be very similar, if not identical, to p57 (Hellen et al., 1993), a protein required for cap-independent translation (Jang & Wimmer, 1990). Previous cross-linking results with endogenous pPTB/p57 (Jang & Wimmer, 1990; G. W. Witherell and E. Wimmer, unpublished results) do not, however, correlate well with the cross-linking and filter binding results of purified pPTB presented here. The addition of HeLa extract to purified pPTB inhibited pPTB binding to some RNAs, an observation suggesting that purified pPTB can bind strongly to RNA fragments which it cannot bind when presented in a mixture containing other HeLa cytoplasmic peptides. Thus, differences between binding specificity with purified and crude pPTB are likely due to the presence of other factors in the extract which alter the binding properties of pPTB, thereby increasing the apparent RNA binding specificity of the protein. Changes in the binding specificity and solution properties of the R17 coat protein–translational operator interaction have also been observed and shown to be due to the formation of a ribonucleoprotein particle containing the R17 coat protein (Beckett et al., 1988; Witherell et al., 1990). Interestingly, incubation of the EMCV IRES with a cell extract also results in formation of a 20S ribonucleoprotein particle (S. K. Jang and E. Wimmer, unpublished results). The EMCV IRES may thus form a ribonucleoprotein complex containing pPTB and other proteins such that the binding properties of pPTB in the complex are not reflected by the binding properties of the purified protein.

The solution properties of pPTB binding to four IRES fragments and the full-length IRES indicate that binding is optimal at low pH, low ionic strength, and high temperatures for each RNA. Similar solution properties have been observed for pPTB cross-linking to a 61-nt-long RNA which encompasses the polypyrimidine tract and lariat branch site of a β-globin intron (Wang & Pederson, 1990). The pPTB–RNA interaction has a large favorable ΔS which is partially offset by a small unfavorable ΔH. Similar thermodynamic binding

properties have been observed for other protein–nucleic acid interactions including the *lac* repressor–operator (Riggs et al., 1970), tRNA synthetase–tRNA (Lam & Schimmel, 1975), ribosomal protein S8–16S rRNA (Mougel et al., 1986), *Hin*fI restriction enzyme–DNA (Frankel et al., 1985), and S4 ribosomal protein α–mRNA (Deckman et al., 1987). A favorable ΔS generally results from the formation of ionic or hydrophobic interactions while an unfavorable ΔH generally results from disruption of hydrogen bonds or van der Waals contacts (Beaudette & Langerman, 1980). The ionic strength dependence of pPTB binding indicates that as many as four ion pairs are formed between pPTB and the RNA upon binding. Ionic interactions however account for less than 35% of the total binding energy. The remaining entropic binding energy could therefore come from either conformational changes of the protein or RNA upon binding or the formation of hydrophobic interactions between pPTB proteins, allowing for the possibility that pPTB binds RNA as a multimer. pPTB does not, however, appear to bind cooperatively since the binding data fit a simple bimolecular noncooperative binding curve.

The ability of pPTB to bind the full-length IRES and IRES fragments 1, 7, 8, and 9 with similar affinity, pH dependence, salt dependence, and temperature dependence suggests that each RNA is bound by a similar or identical mechanism, likely involving the same types of RNA–protein contacts. The likelihood that pPTB binds each RNA by a similar mechanism suggests that RNA fragments which bind pPTB share a common positive binding determinant or lack a specific negative binding determinant. The mere presence of a 10-nt or longer polypyrimidine tract was neither sufficient nor necessary for pPTB binding, and no correlation was observed between the length of a polypyrimidine tract in an RNA and the RNA binding affinity. This is in agreement with previous results suggesting that pPTB recognition is not simply determined by the presence of a polypyrimidine tract, since polyuridine was unable to compete efficiently for pPTB binding (Garcia-Blanco et al., 1989). In a separate study, an RNA lacking a 10-nt-long polypyrimidine tract was able to bind pPTB efficiently, suggesting that pPTB binding cannot be predicted solely on the basis of pyrimidine content (Mulligan et al., 1992). The lack of sequence specificity shown here, the ability of pPTB to bind DNA (Wang & Pederson, 1990), and the unfavorable ΔH suggests that binding specificity is not determined by the formation of hydrogen bonds with functional groups on nucleotide bases or with 2′-OH groups. Instead, we propose that pPTB recognizes a common secondary structure present in RNAs that bind pPTB and absent in those that do not.

We have used computer algorithms of Jaeger and Zuker (Zuker, 1989; Jaeger et al., 1989, 1990) in an attempt to predict the secondary structures of the various IRES RNA fragments (Figure 3). Suboptimal foldings within 2 kcal of the optimal folding were found for many of these fragments. The structures shown in Figure 3 are therefore only one possibility of how the RNA is actually folded in solution. This must be kept in mind when the significance of binding results is considered. Most of the RNA fragments which bind pPTB strongly (fragments 1, 2, 6, 8–11, 14, and 16) contain 5-nt or longer single-stranded bulges or spacers linking two helices, referred to as a helix–ssRNA–helix motif. Although the other two fragments which bind strongly (fragments 3 and 7) lack the helix–ssRNA–helix motif in their thermodynamicly most stable structure, the motif is present in suboptimal foldings of these fragments (within 1 kcal of the optimal folding) in which the 3′-ends of the RNAs are folded into small stem–loops. Other fragments which lack this motif (fragments 4, 5, 12, 13, and 15) do not bind pPTB efficiently. Although the three shortest RNAs tested (fragments 4, 5, and 13) are unable to bind efficiently, there is no general correlation between the length of an RNA and its affinity for pPTB (Figure 3 and Table I). It is thus possible that both single-stranded polypyrimidine tracts and constrained single-stranded regions between helices assume similar secondary structures which pPTB recognizes. Presumably, these structures could orient the phosphate backbone in such a way that four specific ionic recognition sites for pPTB binding are presented. Specific protein–phosphate interactions have been shown to be important for the R17 coat protein–translational operator interaction (Milligan & Uhlenbeck, 1989). The ability of RNA binding proteins such as HIV *tat* (Weeks & Crothers, 1991), HIV *rev* (Bartel et al., 1991), IRE binding protein (Bettany et al., 1992), tRNA synthetases (Schimmel, 1989), and RNA bacteriophage coat proteins (Witherell et al., 1991) to recognize RNA structural features is well characterized.

The role of pPTB in either cap-independent translation or nuclear splicing has not yet been determined. With both IRES RNA fragments described here and pre-mRNA fragments (Gil et al., 1993), the binding specificity of pPTB is reduced upon purification of the protein. These results suggest that pPTB interacts with other factors which alter its binding specificity. Thus pPTB could play a role in site selection as part of a larger complex, or alternatively, pPTB could be required primarily for complex assembly, binding RNA only after the target site has been selected by other factors. The role of pPTB in cap-independent translation and the ability of associated proteins to alter the binding affinity of pPTB to the EMCV IRES is currently being investigated.

ACKNOWLEDGMENT

We thank C. Schultz-Witherell for technical assistance, Dr. A. Jacobson for help in computer-aided RNA folding, Dr. J. Dunn for providing T7 RNA polymerase, and C. Helmke for photographic work.

REFERENCES

Bachman, B. (1987) in *Escherichia coli and Salmonella typhimurium: Cellular and Molecular Biology* (Neidhardt, F. C., et al., Eds.) pp 1190–1219, American Society for Microbiology, Washington, DC.

Bartel, D. P., Zapp, M. L., Green M. R., & Szostak J. W. (1991) *Cell 67*, 529–536.

Beaudette, N. V., & Langerman, N. (1980) *Crit. Rev. Biochem. 9*, 145–170.

Beckett, D., Wu, H.-N., & Uhlenbeck, O. C. (1988) *J. Mol. Biol. 204*, 939–947.

Bettany, A. J., Eisenstein, R. S., & Munro, H. N. (1992) *J. Biol. Chem. 267*, 16531–16537.

Borovjagin, A. V., Ezrokhi, M. V., Rostapshov, V. M., Ugarova, T. Y., Bystrova, T. F., & Shatsky, I. N. (1991) *Nucleic Acids Res. 19*, 4999–5005.

Brown, E. A., Day, S. P., Jansen, R. W., & Lemon, S. M. (1991) *J. Virol. 65*, 5828–5838.

Carey, J., & Uhlenbeck, O. C. (1983) *Biochemistry 22*, 2610–2614.

Deckman, I. C., Draper, D. E., & Thomas, M. S. (1987) *J. Mol. Biol. 196*, 313–322.

Duke, G. M., Hoffman, M. A., & Palmenberg, A. C. (1992) *J. Virol. 66*, 1602–1609.

Frankel, A. D., Ackers, G. K., & Smith, H. O. (1985) *Biochemistry 24*, 3049–3054.

Garcia-Blanco, M. A., Jamison, S. F., & Sharp, P. A. (1989) *Genes Dev. 3*, 1874–1886.
Ghetti, A., Pinol-Roma, S., Michael, W. M., Morandi, C., & Dreyfuss, G. (1992) *Nucleic Acids Res. 20*, 3671–3678.
Gil, A., Sharp, P. A., Jamison, S. F., & Garcia-Blanco, M. A.(1991) *Genes Dev. 5*, 1224–1236.
Hellen, C. U. T., Witherell, G. W., Schmid, M., Shin, S. H., Pestova, T. V., Gill, A., & Wimmer, E. (1993) *Proc. Natl. Acad. Sci. U.S.A.* (in press).
Jaeger, J. A., Turner, D. H., & Zuker, M. (1989) *Proc. Natl. Acad. Sci. U.S.A. 86*, 7706–7710.
Jaeger, J. A., Turner, D. H., & Zuker, M. (1990) *Methods Enzymol. 183*, 281–306.
Jang, S. K., &Wimmer, E. (1990) *Genes Dev. 4*, 1560–1572.
Jang, S. K., Kräusslich, H. G., Nicklin, M. J. H., Duke, G. M., Palmenberg, A. C., & Wimmer, E. (1988) *J. Virol. 62*, 2636–2643.
Jang, S. K., Davies, M. V., Kaufman, R. J., & Wimmer, E. (1989) *J. Virol. 63*, 1651–1660.
Jang, S. K., Pestova, T., Hellen, C. U. T., Witherell, G., & Wimmer, E. (1990) *Enzyme 44*, 292–309.
Kühn, R., Luz, N., & Beck, E. (1990) *J. Virol 64*, 4625–4631.
Laemmli, U. K. (1970) *Nature 227*, 680–685.
Lam, S. S. M., & Schimmel, P. R. (1975) *Biochemistry 14*, 2775–2780.
Lohman, T. M., deHaseth, P. L., & Record, M. T., Jr. (1980) *Biochemistry 19*, 3522–3530.
Luz, N., & Beck, E. (1991) *J. Virol. 65*, 6486–6494.
Macejak, D. G., & Sarnow, P. (1991) *Nature 353*, 90–94.
Milligan, J. F., & Uhlenbeck, O. C. (1989) *Biochemistry 28*, 2849–2855.
Milligan, J. F., Groebe, D. R., Witherell, G. W., & Uhlenbeck, O. C. (1987) *Nucleic Acids Res. 15*, 8783–8798.
Molla, A., Paul, A. V., & Wimmer, E. (1991) *Science 254*, 1647–1651.
Molla, A., Jang, S. K., Paul, A. V., Reuer, Q., & Wimmer, E. (1992) *Nature 356*, 255–257.
Mougel, M., Ehresmann, B., & Ehresmann, C. (1986) *Biochemistry 25*, 2756–2765.
Mulligan, G. J., Guo, W., Wormsley, S., & Helfman, D. M. (1992) *J. Biol. Chem. 267*, 25480–25487.
Nicklin, M. J. H., Kräusslich, H.-G., Toyoda, H., Dunn, J. J., & Wimmer, E. (1987) *Proc. Natl. Acad. Sci. U.S.A. 84*, 4002–4006.
Patton, J. G., Mayer, S. A., Tempst, P., & Nadal-Ginard, B. (1991) *Genes Dev. 5*, 1237–1251.
Pelletier, J., & Sonenberg, N. (1988) *Nature 334*, 320–325.
Pelletier, J., & Sonenberg, N. (1989) *J. Virol. 63*, 441–444.
Pilipenko, E. V., Blinov, V. M., Chernov, B. K., Dimitrieva, T. M., & Agol, V. I. (1989) *Nucleic Acids Res. 17*, 5701–5711.
Raleigh, E. A., Murray, N. E., Revel, H., Blumenthal, R. M., Westaway, D., Reith, A. D., Rigby, P. W. J., Elhai, J., & Hanahan, D. (1988) *Nucleic Acids Res. 16*, 1563–1575.
Record, M. T., Jr., Lohman, T. M., & de Haseth, P. (1976) *J. Mol. Biol. 107*, 145–158.
Riggs, A. D., Bourgeois, S., & Cohn, M. (1970) *J. Mol. Biol. 53*, 401–417.
Sambrook, J., Fritsch, E. F., & Maniatis, T. (1989) *Molecular Cloning*: A Laboratory Manual, 2nd ed., Cold Spring Harbor Laboratory, Cold Spring Harbor, NY.
Sampson, J. R., & Uhlenbeck, O. C. (1988) *Proc. Natl. Acad. Sci. U.S.A. 85*, 1033–1037.
Schimmel, P. (1989) *Biochemistry 28*, 2747–2759.
Tsukiyama-Kohara, K., Iizuka, N., Kohara, M., & Nomoto, A. (1992) *J. Virol. 66*, 1476–1483.
Wang, J., & Pederson, T. (1990) *Nucleic Acids Res. 18*, 5995–6001.
Weeks, K. M., & Crothers, D. M. (1991) *Cell 66*, 577–588.
Witherell, G. W., Wu, H. N., & Uhlenbeck, O. C. (1990) *Biochemistry 29*, 11051–11057.
Witherell, G. W., Gott, J. M., & Uhlenbeck, O. C. (1991) *Prog. Nucleic Acids Res. Mol. Biol. 40*, 185–220.
Zuker, M. (1989) *Science 244*, 48–52.